Effect of the forcing term in the multiple-relaxation-time lattice Boltzmann equation on the shear stress or the strain rate tensor

Zhenhua Chai and T. S. Zhao*

Department of Mechanical Engineering, The Hong Kong University of Science and Technology, Clear Water Bay, Kowloon, Hong Kong SAR, People's Republic of China

(Received 2 February 2012; revised manuscript received 14 June 2012; published 18 July 2012)

In this work, the effect of the forcing term (or external force) in the multiple-relaxation-time lattice Boltzmann equation (MRTLBE) on the shear stress or the strain rate tensor is studied theoretically and numerically. Through a Chapman-Enskog analysis and numerical simulations, we show that the shear stress (or the strain rate tensor) derived from the MRTLBE is second-order accurate in space. We then examine the influence of the forcing term on the shear stress or the strain rate tensor, and demonstrate that the forcing term effect must be included when the shear stress or the strain rate tensor is computed with the nonequilibrium part of the distribution function.

DOI: 10.1103/PhysRevE.86.016705 PACS number(s): 47.11.−j, 44.05.+e

I. INTRODUCTION

The lattice Boltzmann equation (LBE), as a mesoscopic numerical method, has gained significant success in simulating complex fluid flows because of its kinetic characteristics [1–4]. Recently, the LBE has also been extended to the study of blood flows and non-Newtonian fluid flows [5–12], in which one important issue is that the distribution of the shear stress or the strain rate tensor affects the rupture of arterial aneurysms and histological structures of blood vessels [13,14]. Additionally, the shear stressor the strain rate tensor is also a key issue in large eddy simulation of turbulent flows [15], multiphase flows [16], and the polymer and rheology fields [17,18]. For the above reasons, the accurate computation of the shear stress or the strain rate tensor in the LBE is an important issue, and thus has received increasing attention over the past several years [16,19,20]. Generally speaking, the existing strategies for computing the shear stress or the strain rate tensor in the LBE can be classified into two groups: the first is to derive the shear stress or the strain rate tensor directly with the finite difference method [7,20], while the second one is, in the framework of the LBE, to obtain the shear stress or the strain rate tensor from the nonequilibrium part of the distribution function [6,8,9,11,16,19,20]. In the first method, an improper difference scheme to compute the velocity gradient may cause a numerical instability problem or inaccurate numerical results. Moreover, the first method is not suitable for the study of the shear stress or the strain rate tensor of flows in complex geometries. On the other hand, the second method has been proven to be suitable for the study of complex flows because it computes the shear stress or the strain rate tensor locally. For this reason, we focus on the second method in the present work.

Although a number of papers have been published on the study of the shear stress or the strain rate tensor [6,9,11,16,19,20], the forcing term effect on the shear stress or the strain rate tensor in the LBE, especially in the multiple-relaxation-time lattice Boltzmann equation (MRTLBE), has not been studied systematically. In this paper, we study the forcing term effect on the shear stress or the strain rate tensor, and show that this effect must be included in the MRTLBE. In the following, we first present a Chapman-Enskog analysis for derivation of the Navier-Stokes equations and the theoretical expression of the shear stress or the strain rate tensor from the MRTLBE. We then examine the influence of the forcing term on the shear stress or the strain rate tensor, and demonstrate numerically that the forcing term effect must be included when the shear stress or the strain rate tensor is computed with the nonequilibrium part of the distribution function.

II. CHAPMAN-ENSKOG ANALYSIS OF THE MULTIPLE-RELAXATION-TIME LATTICE BOLTZMANN EQUATION

The lattice Boltzmann equation can be viewed as a successor of lattice gas automata [21] or a special discrete form of the continuous Boltzmann equation [22]. Based on the collision operator, the models of the LBE can be classified into the Bhatnagar-Gross-Krook (BGK) model (or the so called single-relaxation-time model) [23] and the generalized lattice Boltzmann model [or multiple-relaxation-time (MRT) model] [24,25]. Here we regard the LBE coupling with the MRT model as the MRTLBE. In the present work, we focus on the MRT model for its superiority over the BGK model in studying single-phase and multiphase flows [25–27].

A. Hydrodynamic equations of the multiple-relaxation-time lattice Boltzmann model

For simplicity, we focus on the multiple-relaxation-time lattice Boltzmann equation in the two-dimensional space only. The evolution equation of the MRTLBE coupling the forcing term reads as [24–29]

$$f_i(\mathbf{x}+\mathbf{c}_i\delta t, t+\delta t) - f_i(\mathbf{x},t) = \Omega_i + \delta t F_i', \tag{1}$$

where Ω_i is the collision operator and defined by

$$\Omega_i = -(\mathbf{M}^{-1}\mathbf{S}\mathbf{M})_{ij}\left[f_j(\mathbf{x},t) - f_j^{(\mathrm{eq})}(\mathbf{x},t)\right]. \tag{2}$$

f_i is the density distribution function associated with the molecular velocity $\mathbf{c}_i$ at position $\mathbf{x}$ and time t, and satisfies

*Corresponding author: metzhao@ust.hk

the following equations:

$$\rho = \sum_i f_i, \tag{3}$$

$$\rho \mathbf{u} = \sum_i \mathbf{c}_i f_i + \frac{\delta t}{2}\mathbf{F}, \tag{4}$$

where $\mathbf{F} = (F_x, F_y)$ represents the external force. F_i' is the discrete forcing term accounting for the external force $\mathbf{F}$ and defined as [28,29]

$$\mathbf{F}' = \mathbf{M}^{-1}\left(\mathbf{I} - \frac{\mathbf{S}}{2}\right)\mathbf{M}\tilde{\mathbf{F}}, \tag{5}$$

where $\mathbf{I}$ is the unit matrix, and $\mathbf{F}' = (F_0', F_1', \ldots, F_b')^\top$ with b representing the number of discrete velocities; $\tilde{\mathbf{F}} = (\tilde{F}_0, \tilde{F}_1, \ldots, \tilde{F}_b)^\top$, and is defined by

$$\tilde{F}_i = w_i\left[\frac{\mathbf{c}_i \cdot \mathbf{F}}{c_s^2} + \frac{(\mathbf{uF} + \mathbf{Fu}) : (\mathbf{c}_i\mathbf{c}_i - c_s^2\mathbf{I})}{2c_s^4}\right]. \tag{6}$$

It should be noted that, if all elements of $\mathbf{S}$ are equal to each other, the MRT model will reduce to the BGK model, and simultaneously, the forcing term proposed for the BGK model [30] can also be derived from Eq. (5).

A lattice Boltzmann model with q velocities in d-dimensional space is usually denoted as a DdQq model. In the D2Q9 model [23], the discrete velocities $\mathbf{c}_i$ in Eq. (1) are given by

$$\mathbf{c}_i = \begin{cases} (0,0), & i = 0, \\ (\cos[(i-1)\pi/2], \sin[(i-1)\pi/2])c, & i = 1\text{–}4, \\ \{\cos[(2i-9)\pi/4], \sin[(2i-9)\pi/4]\}\sqrt{2}c, & i = 5\text{–}8, \end{cases} \tag{7}$$

where $c = \delta x/\delta t$ (set to be 1 in this work), with δx and δt representing the lattice spacing and time step, respectively; $f_i^{(\mathrm{eq})}(x,t)$ is the equilibrium distribution function, and defined as

$$f_i^{(\mathrm{eq})} = w_i\rho\left[1 + \frac{\mathbf{c}_i \cdot \mathbf{u}}{c_s^2} + \frac{(\mathbf{c}_i \cdot \mathbf{u})^2}{2c_s^4} - \frac{|\mathbf{u}|^2}{2c_s^2}\right], \tag{8}$$

where $w_0 = 4/9$, $w_{1\text{–}4} = 1/9$, $w_{5\text{–}8} = 1/36$; $c_s = 1/\sqrt{3}$ is the speed of sound. $\mathbf{M}$ is a transformation matrix,

$$\mathbf{M} = \begin{pmatrix} 1 & 1 & 1 & 1 & 1 & 1 & 1 & 1 & 1 \\ -4 & -1 & -1 & -1 & -1 & 2 & 2 & 2 & 2 \\ 4 & -2 & -2 & -2 & -2 & 1 & 1 & 1 & 1 \\ 0 & 1 & 0 & -1 & 0 & 1 & -1 & -1 & 1 \\ 0 & -2 & 0 & 2 & 0 & 1 & -1 & -1 & 1 \\ 0 & 0 & 1 & 0 & -1 & 1 & 1 & -1 & -1 \\ 0 & 0 & -2 & 0 & 2 & 1 & 1 & -1 & -1 \\ 0 & 1 & -1 & 1 & -1 & 0 & 0 & 0 & 0 \\ 0 & 0 & 0 & 0 & 0 & 1 & -1 & 1 & -1 \end{pmatrix}, \tag{9}$$

which can be used to project the distribution function f_i and equilibrium distribution function $f_i^{(\mathrm{eq})}$ in velocity space onto macroscopic variables in the moment space,

$$\begin{aligned} \mathbf{m} &:= \mathbf{Mf} \\ &= \left(\rho, e, \varepsilon, \rho u_x - \frac{\delta t}{2}F_x, q_x, \rho u_y - \frac{\delta t}{2}F_y, q_y, p_{xx}, p_{xy}\right)^\top, \end{aligned} \tag{10}$$

$$\begin{aligned} \mathbf{m}^{(\mathrm{eq})} &:= \mathbf{Mf}^{(\mathrm{eq})} \\ &= \left(\rho, e^{(\mathrm{eq})}, \varepsilon^{(\mathrm{eq})}, \rho u_x, q_x^{(\mathrm{eq})}, \rho u_y, q_y^{(\mathrm{eq})}, p_{xx}^{(\mathrm{eq})}, p_{xy}^{(\mathrm{eq})}\right)^\top, \end{aligned} \tag{11}$$

where $\mathbf{f} = (f_0, \ldots, f_8)^\top$ and $\mathbf{f}^{(\mathrm{eq})} = (f_0^{(\mathrm{eq})} \ldots, f_8^{(\mathrm{eq})})^\top$. The equilibrium variables of the nonconserved moments $e^{(\mathrm{eq})}$, $\varepsilon^{(\mathrm{eq})}$, $q_x^{(\mathrm{eq})}$, $q_y^{(\mathrm{eq})}$, $p_{xx}^{(\mathrm{eq})}$, and $p_{xy}^{(\mathrm{eq})}$ can be derived from Eq. (11),

$$e^{(\mathrm{eq})} = -2\rho + 3\rho|\mathbf{u}|^2, \tag{12a}$$

$$\varepsilon^{(\mathrm{eq})} = \rho - 3\rho|\mathbf{u}|^2, \tag{12b}$$

$$q_x^{(\mathrm{eq})} = -\rho u_x, \tag{12c}$$

$$q_y^{(\mathrm{eq})} = -\rho u_y, \tag{12d}$$

$$p_{xx}^{(\mathrm{eq})} = \rho\left(u_x^2 - u_y^2\right), \tag{12e}$$

$$p_{xy}^{(\mathrm{eq})} = \rho u_x u_y. \tag{12f}$$

$\mathbf{S}$ is a non-negative relaxation matrix. To keep the relaxation matrix $\mathbf{S}$ consistent with the moment $\mathbf{m}$, we write it in the following form:

$$\mathbf{S} = \mathrm{diag}(s_\rho, s_e, s_\varepsilon, s_j, s_q, s_j, s_q, s_\nu, s_\nu), \tag{13}$$

where $0 < s_i < 2$.

Note that, in the same fashion as in the BGK model, the evolution process of the MRTLBE also consists of two parts: collision and propagation. However, unlike in the BGK model, the collision including the forcing term effect in the MRT model is executed in momentum space,

$$\begin{aligned} &f_i^+(\mathbf{x},t) \\ &= f_i(\mathbf{x},t) - (\mathbf{M}^{-1}\mathbf{SM})_{ij}\left[f_j(\mathbf{x},t) - f_j^{(\mathrm{eq})}(\mathbf{x},t)\right] + \delta t F_i', \end{aligned} \tag{14}$$

whereas the propagation of the MRT model remains in velocity space,

$$f_i(\mathbf{x} + \mathbf{c}_i\delta t, t + \delta t) = f_i^+(\mathbf{x},t). \tag{15}$$

Clearly, the evolution process of the MRTLBE is involved in the transformation between the momentum space and the velocity space.

In what follows, we present a detailed analysis of the derivation of the Navier-Stokes equations from the MRTLBE. To this end, we first adopt the Chapman-Enskog analysis, and expand the density distribution function, the derivatives of time and space, and the external force as

$$f_i = f_i^{(0)} + \epsilon f_i^{(1)} + \epsilon^2 f_i^{(2)} + \cdots, \tag{16a}$$

$$\partial_t = \epsilon\partial_{t_1} + \epsilon^2\partial_{t_2}, \tag{16b}$$

$$\partial_\alpha = \epsilon\partial_{\alpha_1}, \tag{16c}$$

$$\mathbf{F} = \epsilon\mathbf{F}_1, \tag{16d}$$

where $\mathbf{F}_1 = (F_{x1}, F_{y1})$. Substituting the above expansions into Eq. (1), we can obtain the zero-, first-, and

second-order equations in ϵ,

$$\epsilon^0 : f_i^{(0)} = f_i^{(\mathrm{eq})}, \tag{17a}$$

$$\epsilon^1 : D_{1i} f_i^{(0)} = -\frac{1}{\delta t}(\mathbf{M}^{-1}\mathbf{S}\mathbf{M})_{ij} f_j^{(1)} + \left[\mathbf{M}^{-1}\left(\mathbf{I} - \frac{\mathbf{S}}{2}\right)\mathbf{M}\right]_{ij} \tilde{F}_j^1, \tag{17b}$$

$$\epsilon^2 : \partial_{t_2} f_i^{(0)} + D_{1i} f_i^{(1)} + \frac{\delta t}{2} D_{1i}^2 f_i^{(0)} = -\frac{1}{\delta t}(\mathbf{M}^{-1}\mathbf{S}\mathbf{M})_{ij} f_j^{(2)}, \tag{17c}$$

where $D_{1i} = \partial_{t_1} + \mathbf{c}_{i\alpha}\partial_{\alpha_1}$ and $\tilde{F}_i^1 = w_i[\frac{\mathbf{c}_i\cdot\mathbf{F}_1}{c_s^2} + \frac{(\mathbf{u}\mathbf{F}_1+\mathbf{F}_1\mathbf{u}):(\mathbf{c}_i\mathbf{c}_i - c_s^2\mathbf{I})}{2c_s^4}]$.

If we rewrite Eqs. (17) in the vector form and multiply the matrix $\mathbf{M}$ on both sides of them, the corresponding equations in the moment space can be easily derived,

$$\epsilon^0 : \mathbf{m}^{(0)} = \mathbf{m}^{(\mathrm{eq})}, \tag{18a}$$

$$\epsilon^1 : \tilde{\mathbf{D}}_1\mathbf{m}^{(0)} = -\mathbf{S}'\mathbf{m}^{(1)} + \left(\mathbf{I} - \frac{\mathbf{S}}{2}\right)\mathbf{M}\tilde{\mathbf{F}}^1, \tag{18b}$$

$$\epsilon^2 : \partial_{t_2}\mathbf{m}^{(0)} + \tilde{\mathbf{D}}_1\left(\mathbf{I} - \frac{\mathbf{S}}{2}\right)\mathbf{m}^{(1)} + \frac{\delta t}{2}\tilde{\mathbf{D}}_1\left(\mathbf{I} - \frac{\mathbf{S}}{2}\right)\mathbf{M}\tilde{\mathbf{F}}^1 = -\mathbf{S}'\mathbf{m}^{(2)}, \tag{18c}$$

where $\mathbf{S}' = \mathbf{S}/\delta t$, $\tilde{\mathbf{D}}_1 = \mathbf{M}\mathbf{D}_1\mathbf{M}^{-1}$, and $\mathbf{D}_1 = \partial_{t_1}\mathbf{I} + \partial_{\alpha_1}\mathrm{diag}(\mathrm{c}_{0\alpha},\mathrm{c}_{1\alpha},...,\mathrm{c}_{8\alpha})$. Based on Eqs. (10) and (11), one can find that the elements of $\mathbf{m}^{(1)}$ corresponding to the conservative variables ρ and $\rho\mathbf{u}$ are zero and $-\delta t\mathbf{F}_1/2$, so we can further rewrite Eq. (18) as

$$\partial_{t_1}\begin{pmatrix}\rho\\ -2\rho+3\rho|\mathbf{u}|^2\\ \rho-3\rho|\mathbf{u}|^2\\ \rho u_x\\ -\rho u_x\\ \rho u_y\\ -\rho u_y\\ \rho u_x^2-\rho u_y^2\\ \rho u_x u_y\end{pmatrix} + \partial_{x_1}\begin{pmatrix}\rho u_x\\ 0\\ -\rho u_x\\ \frac{\rho}{3}+\rho u_x^2\\ -\frac{\rho}{3}-\rho u_x^2+\rho u_y^2\\ \rho u_x u_y\\ \rho u_x u_y\\ \frac{2\rho u_x}{3}\\ \frac{\rho u_y}{3}\end{pmatrix} + \partial_{y_1}\begin{pmatrix}\rho u_y\\ 0\\ -\rho u_y\\ \rho u_x u_y\\ \rho u_x u_y\\ \frac{\rho}{3}+\rho u_y^2\\ -\frac{\rho}{3}+\rho u_x^2-\rho u_y^2\\ -\frac{2\rho u_y}{3}\\ \frac{\rho u_x}{3}\end{pmatrix} = \begin{pmatrix}0\\ -s_e' e^{(1)}\\ -s_\varepsilon'\varepsilon^{(1)}\\ \frac{\delta t}{2}s_j' F_{x1}\\ -s_q' q_x^{(1)}\\ \frac{\delta t}{2}s_j' F_{y1}\\ -s_q' q_y^{(1)}\\ -s_\nu' p_{xx}^{(1)}\\ -s_\nu' p_{xy}^{(1)}\end{pmatrix} + \begin{pmatrix}0\\ 6\left(1-\frac{s_e}{2}\right)\mathbf{u}\cdot\mathbf{F}_1\\ -6\left(1-\frac{s_\varepsilon}{2}\right)\mathbf{u}\cdot\mathbf{F}_1\\ \left(1-\frac{s_j}{2}\right)F_{x1}\\ -\left(1-\frac{s_q}{2}\right)F_{x1}\\ \left(1-\frac{s_j}{2}\right)F_{y1}\\ -\left(1-\frac{s_q}{2}\right)F_{y1}\\ 2\left(1-\frac{s_\nu}{2}\right)(u_x F_{x1}-u_y F_{y1})\\ \left(1-\frac{s_\nu}{2}\right)(u_x F_{y1}+u_y F_{x1})\end{pmatrix}. \tag{19}$$

Similarly, we can also derive the second-order hydrodynamic equations in ϵ, but we present only the ones corresponding to the conservative variables ρ and $\rho\mathbf{u}$,

$$\partial_{t_2}\rho = 0, \tag{20a}$$

$$\begin{aligned}&\partial_{t_2}(\rho u_x) - \frac{\delta t}{2}\partial_{t_1}\left[\left(1-\frac{s_j}{2}\right)F_{x1}\right] + \frac{1}{6}\partial_{x_1}\left[\left(1-\frac{s_e}{2}\right)e^{(1)}\right] + \frac{1}{2}\partial_{x_1}\left[\left(1-\frac{s_\nu}{2}\right)p_{xx}^{(1)}\right] + \partial_{y_1}\left[\left(1-\frac{s_\nu}{2}\right)p_{xy}^{(1)}\right]\\ &+\frac{\delta t}{2}\left\{\partial_{t_1}\left[\left(1-\frac{s_j}{2}\right)F_{x1}\right] + \partial_{x_1}\left[\frac{s_\nu}{2}(u_y F_{y1}-u_x F_{x1}) - \frac{s_e}{2}(u_x F_{x1}+u_y F_{y1}) + 2u_x F_{x1}\right]\right.\\ &\left.+\partial_{y_1}\left[\left(1-\frac{s_\nu}{2}\right)(u_x F_{y1}+u_y F_{x1})\right]\right\} = 0,\end{aligned} \tag{20b}$$

$$\begin{aligned}&\partial_{t_2}(\rho u_y) - \frac{\delta t}{2}\partial_{t_1}\left[\left(1-\frac{s_j}{2}\right)F_{y1}\right] + \partial_{x_1}\left[\left(1-\frac{s_\nu}{2}\right)p_{xy}^{(1)}\right] - \frac{1}{2}\partial_{y_1}\left[\left(1-\frac{s_\nu}{2}\right)p_{xx}^{(1)}\right] + \frac{1}{6}\partial_{y_1}\left[\left(1-\frac{s_e}{2}\right)e^{(1)}\right]\\ &+\frac{\delta t}{2}\left\{\partial_{t_1}\left[\left(1-\frac{s_j}{2}\right)F_{y1}\right] + \partial_{x_1}\left[\left(1-\frac{s_\nu}{2}\right)(u_x F_{y1}+u_y F_{x1})\right]\right.\\ &\left.+\partial_{y_1}\left[\frac{s_\nu}{2}(u_x F_{x1}-u_y F_{y1}) - \frac{s_e}{2}(u_x F_{x1}+u_y F_{y1}) + 2u_y F_{y1}\right]\right\} = 0.\end{aligned} \tag{20c}$$

Under the incompressible condition [the term $O(|\mathbf{u}|^3)$ is neglected] and with the aid of Eq. (19), we can obtain the following equations for $e^{(1)}$, $p_{xx}^{(1)}$ and $p_{xy}^{(1)}$:

$$-s_e' e^{(1)} = 6p\left(\partial_{x_1}u_x + \partial_{y_1}u_y\right) + 3s_e\mathbf{u}\cdot\mathbf{F}_1, \tag{21a}$$

$$-s_\nu' p_{xx}^{(1)} = 2p\left(\partial_{x_1}u_x - \partial_{y_1}u_y\right) + s_\nu(u_x F_{x1} - u_y F_{y1}), \tag{21b}$$

$$-s_\nu' p_{xy}^{(1)} = p\left(\partial_{x_1}u_y + \partial_{y_1}u_x\right) + \frac{s_\nu}{2}(u_x F_{y1} + u_y F_{x1}), \tag{21c}$$

where $p = \rho c_s^2 = \rho/3$. Substituting Eq. (21) into Eq. (20), the second-order hydrodynamic equations in ϵ can be derived,

$$\partial_{t_2}\rho = 0, \tag{22a}$$

$$\partial_{t_2}(\rho u_x) = \partial_{x_1}\left[\rho\nu\left(\partial_{x_1}u_x - \partial_{y_1}u_y\right) + \rho\xi\left(\partial_{x_1}u_x + \partial_{y_1}u_y\right)\right] + \partial_{y_1}\left[\rho\nu\left(\partial_{x_1}u_y + \partial_{y_1}u_x\right)\right], \tag{22b}$$

$$\partial_{t_2}(\rho u_y) = \partial_{x_1}\left[\rho\nu\left(\partial_{x_1}u_y + \partial_{y_1}u_x\right)\right] + \partial_{y_1}\left[\rho\nu\left(\partial_{y_1}u_y - \partial_{x_1}u_x\right) + \rho\xi\left(\partial_{x_1}u_x + \partial_{y_1}u_y\right)\right], \tag{22c}$$

where ν and ξ are the kinematic and bulk viscosities and given by

$$\nu = c_s^2\left(\frac{1}{s_\nu} - \frac{1}{2}\right)\delta t, \quad \xi = c_s^2\left(\frac{1}{s_e} - \frac{1}{2}\right)\delta t. \tag{23}$$

Combining the results at the t_1 and t_2 time scales, i.e., Eqs. (19) and (22), we can obtain the following Navier-Stokes equations:

$$\partial_t\rho + \nabla\cdot(\rho\mathbf{u}) = 0, \tag{24a}$$

$$\partial_t(\rho\mathbf{u}) + \nabla\cdot(\rho\mathbf{u}\mathbf{u}) = -\nabla p + \nabla\cdot\boldsymbol{\tau} + \mathbf{F}, \tag{24b}$$

where $\boldsymbol{\tau}$ is the shear stress and defined by

$$\boldsymbol{\tau} = 2\rho\nu\dot{\mathbf{e}} + \rho(\xi - \nu)(\nabla\cdot\mathbf{u})\mathbf{I}, \tag{25}$$

for incompressible flows. Equation (25) can be further simplified using $\boldsymbol{\tau} = 2\rho\nu\dot{\mathbf{e}}$, where $\dot{\mathbf{e}} = \frac{1}{2}[\nabla\mathbf{u} + (\nabla\mathbf{u})^\top]$ is the strain rate tensor.

Finally, let us focus on discussing the relaxation matrix $\mathbf{S}$. In the process of deriving the Navier-Stokes equations, it is found that the relaxation factors s_ρ and s_j have no influence on the macroscopic hydrodynamic equations, and thus their values can be chosen arbitrarily. For simplicity, the relation $s_\rho = s_j = 0$ will be used in the present simulations. In addition to s_ν, s_ρ, and s_j, there are three adjustable parameters s_e, s_ε, and s_q. The relaxation parameter s_e is related to the bulk viscosity ξ and usually adjusted to enhance the numerical stability of the MRT model; similarly, s_ε can also be changed to improve the numerical stability of the MRT model [26]. Compared to s_e and s_ε, the parameter s_q is usually related to implementation of boundary conditions and can be used to improve the accuracy of the MRT model [26,29,31]. In fact, numerical results in some previous works have shown that more freedom in choosing the relaxation factors indeed ensures that the MRT model possesses more potential than the BGK model for studying some problems [26–29,31,32].

B. Shear stress and strain rate tensor in the multiple-relaxation-time lattice Boltzmann equation

In this section, we focus on discussing the computation of the shear stress or the strain rate tensor in the framework of the MRTLBE with the nonequilibrium part of the distribution function. Based on Eqs. (17b) and (19), we can obtain

$$\begin{aligned}
&-\frac{1}{\delta t}\sum_i c_{i_\alpha}c_{i_\beta}(\mathbf{M}^{-1}\mathbf{S}\mathbf{M})_{ij}f_j^{(1)} \\
&= \sum_i c_{i_\alpha}c_{i_\beta}D_{1i}f_i^{(0)} - \sum_i c_{i_\alpha}c_{i_\beta}\left[\mathbf{M}^{-1}\left(\mathbf{I} - \frac{\mathbf{S}}{2}\right)\mathbf{M}\right]_{ij}\tilde{F}_j^1 \\
&= \partial_{t_1}\left(\rho c_s^2\delta_{\alpha\beta} + \rho u_\alpha u_\beta\right) + \partial_{\gamma_1}\left[\rho c_s^2(u_\alpha\delta_{\beta\gamma} + u_\beta\delta_{\alpha\gamma} + u_\gamma\delta_{\alpha\beta})\right] - \sum_i c_{i_\alpha}c_{i_\beta}\left[\mathbf{M}^{-1}\left(\mathbf{I} - \frac{\mathbf{S}}{2}\right)\mathbf{M}\right]_{ij}\tilde{F}_j^1,
\end{aligned} \tag{26}$$

$$\partial_{t_1}\rho = -\partial_{\gamma_1}(\rho u_\gamma), \tag{27}$$

$$\partial_{t_1}(\rho u_\alpha u_\beta) = -u_\beta\partial_{\alpha_1}p - u_\alpha\partial_{\beta_1}p + u_\beta F_{\alpha 1} + u_\alpha F_{\beta 1}. \tag{28}$$

Substituting Eqs. (27) and (28) into Eq. (26), we obtain

$$\begin{aligned}
&-\frac{1}{\delta t}\sum_i c_{i_\alpha}c_{i_\beta}(\mathbf{M}^{-1}\mathbf{S}\mathbf{M})_{ij}f_j^{(1)} \\
&= \rho c_s^2\left(\partial_{\beta_1}u_\alpha + \partial_{\alpha_1}u_\beta\right) + F_{\alpha 1}u_\beta + u_\alpha F_{\beta 1} - \sum_i c_{i_\alpha}c_{i_\beta}\left[\mathbf{M}^{-1}\left(\mathbf{I} - \frac{\mathbf{S}}{2}\right)\mathbf{M}\right]_{ij}\tilde{F}_j^1.
\end{aligned} \tag{29}$$

Multiplying ϵ on both sides of Eq. (29) and assuming $\epsilon f_i^{(1)} = f_i^{(\mathrm{neq})} = f_i - f_i^{(\mathrm{eq})}$ to be valid, we can obtain the strain rate tensor

$$\begin{aligned}
\dot{\mathbf{e}} = \frac{1}{2}[\nabla\mathbf{u} + (\nabla\mathbf{u})^\top] &= \frac{\delta t\left\{\sum_i \mathbf{c}_i\mathbf{c}_i\left[\mathbf{M}^{-1}\left(\mathbf{I} - \frac{\mathbf{S}}{2}\right)\mathbf{M}\right]_{ij}\tilde{F}_j - (\mathbf{u}\mathbf{F} + \mathbf{F}\mathbf{u})\right\} - \sum_i \mathbf{c}_i\mathbf{c}_i(\mathbf{M}^{-1}\mathbf{S}\mathbf{M})_{ij}f_j^{(\mathrm{neq})}}{2\rho c_s^2\delta t} \\
&= \frac{[(s_\nu - s_e)(\mathbf{u}\cdot\mathbf{F})\mathbf{I} - s_\nu(\mathbf{u}\mathbf{F} + \mathbf{F}\mathbf{u})]}{4\rho c_s^2} - \frac{\sum_i \mathbf{c}_i\mathbf{c}_i(\mathbf{M}^{-1}\mathbf{S}\mathbf{M})_{ij}f_j^{(\mathrm{neq})}}{2\rho c_s^2\delta t}.
\end{aligned} \tag{30}$$

We can also use Eq. (30) to obtain the shear stress $\boldsymbol{\tau}$,

$$\boldsymbol{\tau} = \frac{\nu\left[(s_\nu - s_e)(\mathbf{u}\cdot\mathbf{F})\mathbf{I} - s_\nu(\mathbf{u}\mathbf{F} + \mathbf{F}\mathbf{u})\right]}{2c_s^2} - \frac{\nu\sum_i \mathbf{c}_i\mathbf{c}_i(\mathbf{M}^{-1}\mathbf{S}\mathbf{M})_{ij}f_j^{(\mathrm{neq})}}{c_s^2\delta t}. \tag{31}$$

The first term on the right hand side of Eqs. (30) and (31) is considered as the forcing term effect on the strain rate tensorand the shear stress. In addition, we also would like to point out that, if the relaxation factors in the MRT model are taken to be a single value s_{BGK}, the strain rate tensor and shear stress in the BGK model can be

obtained:

$$\dot{\mathbf{e}} = \frac{1}{2}[\nabla\mathbf{u} + (\nabla\mathbf{u})^{\top}] = -\frac{s_{\mathrm{BGK}}}{4\rho c_s^2 \delta t}\left[\delta t(\mathbf{uF} + \mathbf{Fu}) + 2\sum_i \mathbf{c}_i\mathbf{c}_i f_i^{(\mathrm{neq})}\right], \quad (32)$$

$$\boldsymbol{\tau} = -\frac{2 - s_{\mathrm{BGK}}}{4}\left[\delta t(\mathbf{uF} + \mathbf{Fu}) + 2\sum_i \mathbf{c}_i\mathbf{c}_i f_i^{(\mathrm{neq})}\right]. \quad (33)$$

It is noticed that the forcing term effect has been considered in the computation of shear stress in the BGK model [16,19,20]. For instance, Gross *et al*. adopted the force scheme proposed by Ladd and Verberg [19],

$$F_i' = w_i\left[\frac{\mathbf{c}_i\cdot\mathbf{F}}{c_s^2} + \frac{(\mathbf{uF} + \mathbf{Fu}) : (\mathbf{c}_i\mathbf{c}_i - c_s^2\mathbf{I})}{2c_s^4}\right], \quad (34)$$

while Krüger *et al*. used a simple one [20],

$$F_i' = w_i\frac{\mathbf{c}_i\cdot\mathbf{F}}{c_s^2}. \quad (35)$$

However, as pointed out elsewhere [30], none of the above-mentioned schemes enables correct hydrodynamic equations to be recovered. To derive the correct Navier-Stokes equations, one should use the following force scheme for the BGK model:

$$F_i' = w_i\left(1 - \frac{s_{\mathrm{BGK}}}{2}\right)\left[\frac{\mathbf{c}_i\cdot\mathbf{F}}{c_s^2} + \frac{(\mathbf{uF} + \mathbf{Fu}) : (\mathbf{c}_i\mathbf{c}_i - c_s^2\mathbf{I})}{2c_s^4}\right]. \quad (36)$$

C. Convergence of the shear stress or the strain rate tensor in the multiple-relaxation-time lattice Boltzmann equation

Previous studies [2,20] have demonstrated that the velocity and shear stress of the lattice Boltzmann equation can be recovered to those of the Navier-Stokes equations with a second-order accuracy in space, i.e., the global relative errors of velocity ($\mathcal{E}_{\mathbf{u}}$) and shear stress ($\mathcal{E}_{\boldsymbol{\tau}}$) scale with δx^2. In diffusive scaling, the time step and the lattice spacing satisfy the relation $\delta t \propto \delta x^2$, while the Mach number (Ma) linearly scales with the lattice spacing, $\mathrm{Ma} \propto \delta x$ [20]. It follows that the global relative error of the velocity and shear stress are

$$\mathcal{E}_{\mathbf{u}} \propto \mathrm{Ma}^2, \quad \mathcal{E}_{\boldsymbol{\tau}} \propto \mathrm{Ma}^2. \quad (37)$$

Note that above theoretical results have been validated numerically in a recent work [20]. In what follows, we will present an analysis of the convergence of the shear stress and the strain rate tensor in the multiple-relaxation-time lattice Boltzmann equation.

We can first rewrite Eq. (29) in a more complete form,

$$-\frac{1}{\delta t}\sum_i c_{i_\alpha}c_{i_\beta}(\mathbf{M}^{-1}\mathbf{SM})_{ij} f_j^{(1)} = \rho c_s^2\left(\partial_{\beta_1}u_\alpha + \partial_{\alpha_1}u_\beta\right) + F_{\alpha 1}u_\beta + u_\alpha F_{\beta 1} - \sum_i c_{i_\alpha}c_{i_\beta}\left[\mathbf{M}^{-1}\left(\mathbf{I} - \frac{\mathbf{S}}{2}\right)\mathbf{M}\right]_{ij}\tilde{F}_j^1 + E_{1_{\alpha\beta}}, \quad (38)$$

where $E_{1_{\alpha\beta}}$ is considered as the error term neglected in Eq. (29) and can be derived from Eq. (26),

$$E_{1_{\alpha\beta}} = -\partial_{\gamma_1}(\rho u_\alpha u_\beta u_\gamma). \quad (39)$$

Based on the analysis reported elsewhere [20], we can obtain the following result within the diffusive scaling,

$$E_{1_{\alpha\beta}} \propto \mathrm{Ma}^4. \quad (40)$$

The above analysis suggests that the shear stress and the strain rate tensor in the MRTLBE will converge with a second-order accuracy if $f_i^{(1)}$ is known and used in the computation. As pointed out elsewhere [20], however, it is not practical to compute $f_i^{(1)}$ in lattice Boltzmann simulations, which is also the reason why we use $f_i^{(\mathrm{neq})}$ instead of $f_i^{(1)}$ to compute the shear stress and the strain rate tensor with Eqs. (31) and (30).

It should be noted that, compared to Eqs. (26) or (38), the approximate computation of the shear stress or the strain rate tensor [Eqs. (31) or (30)] may bring some additional errors. To check the errors induced by the approximation of $\epsilon f_i^{(1)} \approx f_i^{(\mathrm{neq})}$, we need to evaluate the effect of the higher orders of the nonequilibrium part [$f_i^{(k)}$, $k \geqslant 2$] on the shear stressand the strain rate tensor. But in the following, we restrict our attention to the influence of $f_i^{(2)}$ since the higher orders of the nonequilibrium part [$f_i^{(k)}$, $k > 2$] become less important with increasing order of ϵ. One can use the following equation instead of Eq. (38) to include the effect of the nonequilibrium part to the second order:

$$-\frac{1}{\delta t}\sum_i c_{i_\alpha}c_{i_\beta}(\mathbf{M}^{-1}\mathbf{SM})_{ij} f_j^{(\mathrm{neq})} = \rho c_s^2(\partial_\beta u_\alpha + \partial_\alpha u_\beta) + F_\alpha u_\beta + u_\alpha F_\beta - \sum_i c_{i_\alpha}c_{i_\beta}\left[\mathbf{M}^{-1}\left(\mathbf{I} - \frac{\mathbf{S}}{2}\right)\mathbf{M}\right]_{ij}\tilde{F}_j + \epsilon E_{1_{\alpha\beta}} + \epsilon^2 E_{\epsilon_{\alpha\beta}}, \quad (41)$$

where $E_{\epsilon_{\alpha\beta}}$ is the error caused by the second order of the nonequilibrium part $f_i^{(2)}$ and defined by

$$E_{\epsilon_{\alpha\beta}} = -\frac{1}{\delta t}\sum_i c_{i_\alpha}c_{i_\beta}(\mathbf{M}^{-1}\mathbf{SM})_{ij} f_j^{(2)}. \quad (42)$$

With the help of Eqs. (17b) and (17c), the error $E_{\epsilon_{\alpha\beta}}$ can be expressed as

$$E_{\epsilon_{\alpha\beta}} = E_{\bar{\epsilon}_{\alpha\beta}} + E_{\tilde{\epsilon}_{\alpha\beta}}, \quad (43)$$

where $E_{\bar{\epsilon}_{\alpha\beta}} = \partial_{t_2}\sum_i c_{i_\alpha}c_{i_\beta}f_i^{(0)} = \partial_{t_2}(\rho c_s^2\delta_{\alpha\beta} + \rho u_\alpha u_\beta)$ and $E_{\tilde{\epsilon}_{\alpha\beta}} = \sum_i D_{1i}c_{i_\alpha}c_{i_\beta}[\mathbf{M}^{-1}(\mathbf{I} - \frac{\mathbf{S}}{2})\mathbf{M}]_{ij}[f_j^{(1)} + \frac{\delta t}{2}\tilde{F}_j^1]$.

We first give an evaluation of the term $E_{\bar{\epsilon}_{\alpha\beta}}$, which can be rewritten as the following equation:

$$\begin{aligned} E_{\bar{\epsilon}_{\alpha\beta}} &= \partial_{t_2}\left(\rho c_s^2\delta_{\alpha\beta} + \rho u_\alpha u_\beta\right) \\ &= c_s^2\delta_{\alpha\beta}\partial_{t_2}\rho + u_\alpha\partial_{t_2}(\rho u_\beta) + u_\beta\partial_{t_2}(\rho u_\alpha) - u_\alpha u_\beta\partial_{t_2}\rho \\ &= u_\alpha\partial_{t_2}(\rho u_\beta) + u_\beta\partial_{t_2}(\rho u_\alpha), \end{aligned} \quad (44)$$

where Eq. (22a) has been used. Based on the second-order equations [Eqs. (22b) and (22c)] in ϵ and the fact that $u_\alpha \propto \mathrm{Ma}$ and $\partial_\alpha \propto \mathrm{Ma}$ [20], one can easily find $\partial_{t_2}(\rho u_\alpha) \propto \mathrm{Ma}^3$, which can be substituted into Eq. (44) to derive $E_{\bar{\epsilon}_{\alpha\beta}} \propto \mathrm{Ma}^4$.

To evaluate the second term $E_{\bar{\epsilon}_{\alpha\beta}}$, we introduce a vector $\mathbf{\Psi}$ with nine elements, and use Ψ_i to denote $[(\mathbf{I}-\frac{\mathbf{S}}{2})\mathbf{M}]_{ij}[f_j^{(1)}+\frac{\delta t}{2}\tilde{F}_j^1]$. With the aid of Eq. (19), we can obtain each element of $\mathbf{\Psi}$,

$$\Psi_0 = 0, \tag{45a}$$

$$\Psi_1 = -2\rho\delta t\left(\frac{1}{s_e}-\frac{1}{2}\right)\left(\partial_{x_1}u_x+\partial_{y_1}u_y\right), \tag{45b}$$

$$\Psi_2 = 2\rho\delta t\left(\frac{1}{s_\epsilon}-\frac{1}{2}\right)\left(\partial_{x_1}u_x+\partial_{y_1}u_y\right), \tag{45c}$$

$$\Psi_3 = 0, \tag{45d}$$

$$\Psi_4 = -\delta t\left(\frac{1}{s_q}-\frac{1}{2}\right)\left[\partial_{x_1}\left(\rho u_y^2\right)+2\partial_{y_1}(\rho u_x u_y)\right], \tag{45e}$$

$$\Psi_5 = 0, \tag{45f}$$

$$\Psi_6 = -\delta t\left(\frac{1}{s_q}-\frac{1}{2}\right)\left[2\partial_{x_1}(\rho u_x u_y)+\partial_{y_1}\left(\rho u_x^2\right)\right], \tag{45g}$$

$$\Psi_7 = -\frac{2\rho\delta t}{3}\left(\frac{1}{s_v}-\frac{1}{2}\right)\left(\partial_{x_1}u_x-\partial_{y_1}u_y\right), \tag{45h}$$

$$\Psi_8 = -\frac{\rho\delta t}{3}\left(\frac{1}{s_v}-\frac{1}{2}\right)\left(\partial_{x_1}u_y+\partial_{y_1}u_x\right). \tag{45i}$$

If we recognize the fact that $u_\alpha \propto \mathrm{Ma}$, $\partial_\alpha \propto \mathrm{Ma}$, and $\delta t \propto \delta x^2 \propto \mathrm{Ma}^2$ in diffusive scaling [20], we can find $\Psi_i \propto \mathrm{Ma}^4$ or Ma^5. Substituting Eq. (45) into $E_{\bar{\epsilon}_{\alpha\beta}}$, we can also prove that $E_{\bar{\epsilon}_{\alpha\beta}} = \sum_i D_{1i}c_{i_\alpha}c_{i_\beta}[\mathbf{M}^{-1}(\mathbf{I}-\frac{\mathbf{S}}{2})\mathbf{M}]_{ij}[f_j^{(1)}+\frac{\delta t}{2}\tilde{F}_j^1] \propto \mathrm{Ma}^4$, and thus the absolute error $E_{\epsilon_{\alpha\beta}}$ defined by Eq. (43) is of order Ma^4. The above analysis indicates that the global relative error of the shear stress or the strain rate tensor, as computed from Eqs. (31) or (30), is second-order accurate in Ma or the lattice spacing δx.

III. NUMERICAL RESULTS AND DISCUSSION

In this section, the accuracy of the MRTLBE in computing the velocity and shear stress or strain rate tensor is tested, and the forcing term effect on the shear stress or the strain rate tensor in the MRTLBE is then discussed. Since the MRTLBE is an explicit time-marching method, a large number of time steps are required to reach a steady state when it is used to simulate steady flows. To ensure that our simulation results are for a steady state, the following convergence criterion has been adopted:

$$\frac{\sum_{x,y}|u_x(x,y,t)-u_x(x,y,t-100\delta t)|}{\sum_{x,y}|u_x(x,y,t)|} < \Delta, \tag{46}$$

where Δ is set to be 1.0×10^{-7} in the present work. We note that a similar convergence criterion has also been used in many previous works (e.g., [7]).

A. The accuracy and convergence of the multiple-relaxation-time lattice Boltzmann equation in computing the velocity and shear stress or strain rate tensor

To test the accuracy of the MRTLBE in computing the velocity and shear stress or strain rate tensor, we take the simplified four-roll mill problem, shown in Fig. 1, as an example.

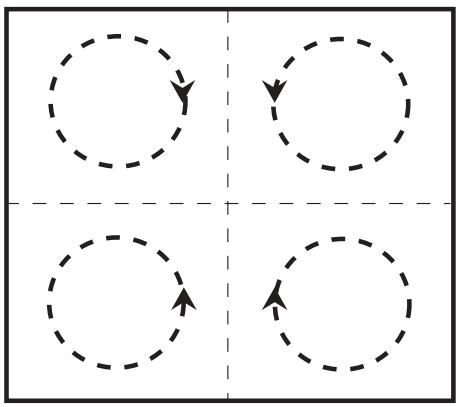

FIG. 1. Schematic of two-dimensional four-roll mill problem.

The geometry of the problem is a two-dimensional periodic box with a size $[0,2\pi]\times[0,2\pi]$. In this tested example, the four cylinders rotate in such a way that an elongational flow is formed in the vicinity of a central stagnation point. In this work, the four rollers are replaced by a body force to drive flow, which can produce four vortices at the locations of the rollers [33]. The purpose for choosing such a problem is twofold. First, the problem has an analytical solution, which is suitable as an accuracy test of numerical methods [33]; and second, the boundary condition of the problem is periodic, which can be used to exclude the boundary effect on the numerical results. Provided that the flow is incompressible (the fluid density ρ_0 is assumed to be a constant, for example, $\rho_0 = 1.0$), and driven by the following acceleration:

$$\begin{aligned} a_x &= u_0^2\sin(x)\cos(x)+2\nu u_0\sin(x)\cos(y),\\ a_y &= u_0^2\sin(y)\cos(y)-2\nu u_0\sin(y)\cos(x), \end{aligned} \tag{47}$$

we can derive analytical solutions for the velocity and shear stress

$$u_x = u_0\sin(x)\cos(y), \tag{48a}$$

$$u_y = -u_0\sin(y)\cos(x), \tag{48b}$$

$$\tau_{xx} = 2\rho_0\nu u_0\cos(x)\cos(y), \tag{48c}$$

$$\tau_{xy} = \tau_{yx} = 0, \tag{48d}$$

$$\tau_{yy} = -2\rho_0\nu u_0\cos(x)\cos(y), \tag{48e}$$

which can also be used to obtain elements of the strain rate tensor $\dot{\mathbf{e}}$.

We performed some numerical experiments to test the accuracy of the MRTLBE in computing the velocity and shear stress, and the results for one case are presented in Figs. 2 and 3, where a lattice size 64×64, which is large enough to derive accurate results, is used. The velocity u_0 in Eq. (47) and the relaxation factor s_v are set to be 0.1 and 1.24, which can also be used to derive the kinematic viscosity $\nu = 0.01$; the other relaxation parameters in Eq. (13) are given as $s_e = s_\varepsilon = 0.8, s_q = 1.9$. As seen from Figs. 2 and 3 (left), the numerical results are in good agreement with analytical solutions. Besides that, Fig. 3 (right) seems to present some obvious differences between the numerical results and analytical solutions, but after a careful observation, one can find that the numerical results are of order 10^{-6}, which is very close to the analytical solution ($\tau_{xy} = 0$). In addition,

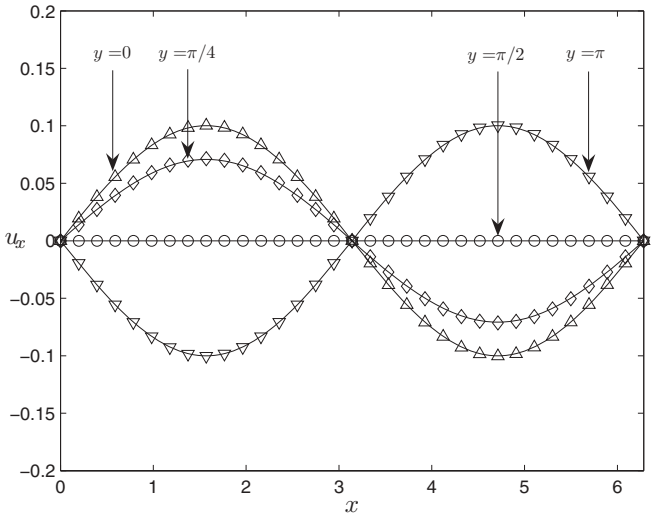

FIG. 2. Profiles of velocity component u_x at different positions (solid lines, analytical results; symbols, numerical results).

the results in Fig. 3 also show that the forcing term effect on the shear stress seems to be invisible; the reason for this observation is as follows. The acceleration $\mathbf{a} = (a_x, a_y)$ given by Eq. (47) can be expressed as

$$\mathbf{a} = \mathbf{u}\cdot\nabla\mathbf{u} - \nu\nabla^2\mathbf{u} = \mathbf{u}\cdot\nabla\mathbf{u} - \frac{1}{3}\left(\frac{1}{s_\nu} - \frac{1}{2}\right)\delta t\nabla^2\mathbf{u}. \quad (49)$$

If we substitute Eq. (49) into Eq. (31) and use the relation $\mathbf{F} = \rho\mathbf{a}$, we find that the terms associated with $\mathbf{F}$ in Eq. (31) have the same order as those we omitted in the process of deriving Eq. (31). For this reason, we can conclude that the forcing term effect on the shear stress can be neglected, and also that the four-roll problem considered here is not a typical problem to reflect the importance of the forcing term effect.

To test the convergence property of the MRTLBE in computing the velocity and shear stress or strain rate tensor, the following global relative error ($\mathcal{E}$) is used, and defined by

$$\mathcal{E}_{u_k} = \frac{\sum_{x,y}|u_{k,n}(x,y) - u_{k,a}(x,y)|}{\sum_{x,y}|u_{k,a}(x,y)|}, \quad (50)$$

$$\mathcal{E}_{\tau_{ij}} = \frac{\sum_{x,y}|\tau_{ij,n}(x,y) - \tau_{ij,a}(x,y)|}{\sum_{x,y}|\tau_{ij,a}(x,y)|}, \quad (51)$$

where $i,j,k = x$ or y, and the subscripts a and n denote analytical and numerical solutions, respectively. We also carried out several numerical simulations with different lattice sizes, ranging from 17×17 to 129×129, and show the results in Fig. 4. In our simulations, the Reynolds number ($\mathrm{Re} = Lu_0/\nu$, $L = 2\pi$) and the relaxation factor s_ν are fixed to be 10 and 1.11, which can be used to derive the desired kinematic viscosity ν. As shown in Fig. 4, we find that, like BGK model [20], the MRT model is also a second-order scheme for computing the velocity and shear stress including or without including the forcing term effect. In addition, for the fixed Reynolds number and relaxation factor s_ν, one can also conclude that the MRT model is second-order accurate in the Mach number ($\mathrm{Ma} = u_0/c_s$) based on the following equation:

$$\frac{\mathrm{Ma}}{\mathrm{Re}} = \frac{\frac{1}{s_\nu} - \frac{1}{2}}{\sqrt{3}N}, \quad (52)$$

where $N = L/\delta x$ is the grid number.

We further tested whether there is any deviation from the second-order convergence of the MRTLBE in computing the velocity and shear stress when the Reynolds number is increased to a critical value at which the numerical method is unstable. To this end, we first derive such a critical Reynolds number ($\mathrm{Re}_c = 50$) for the case of $\delta x = 1/16$ and $s_\nu = 1.11$ where the Mach number is about 0.72, and we then perform several numerical simulations when the Reynolds number and relaxation factor s_ν are fixed to be 50 and 1.11, and present the global relative errors under different grid sizes in Fig. 5.

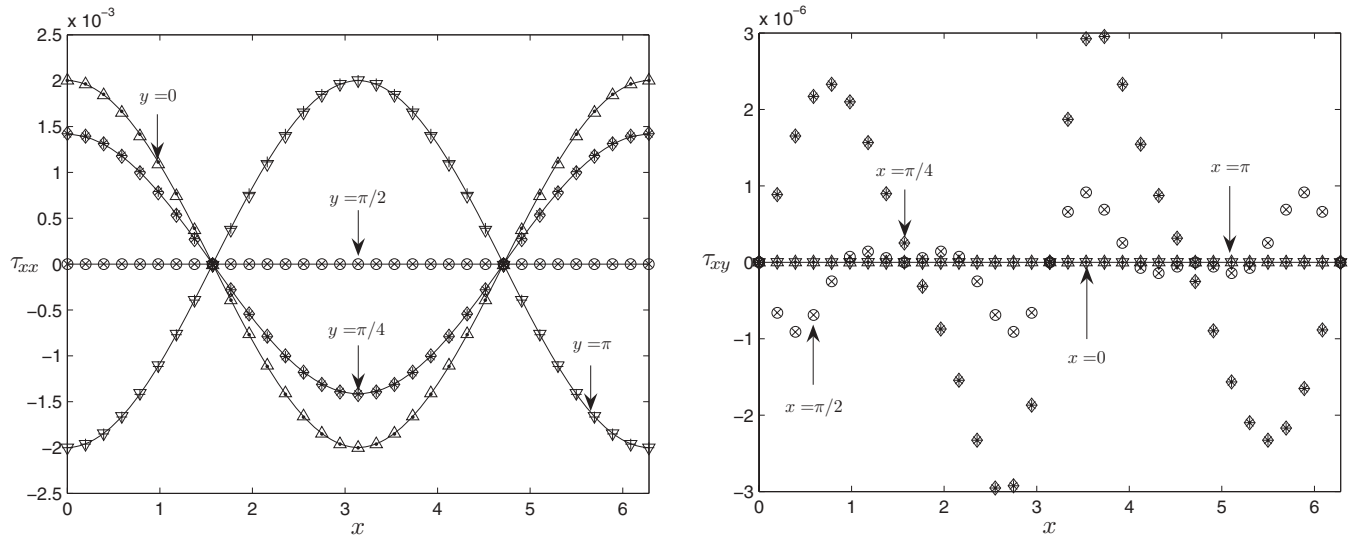

FIG. 3. Profiles of shear stress components τ_{xx} (left) and τ_{xy} (right) at different positions (solid lines are analytical results; symbols $\triangle$, $\diamond$, $\circ$, and $\triangledown$ are numerical results including the forcing term effect; $\bullet$, $*$, $\times$, and $+$ are numerical results without including the forcing term effect).

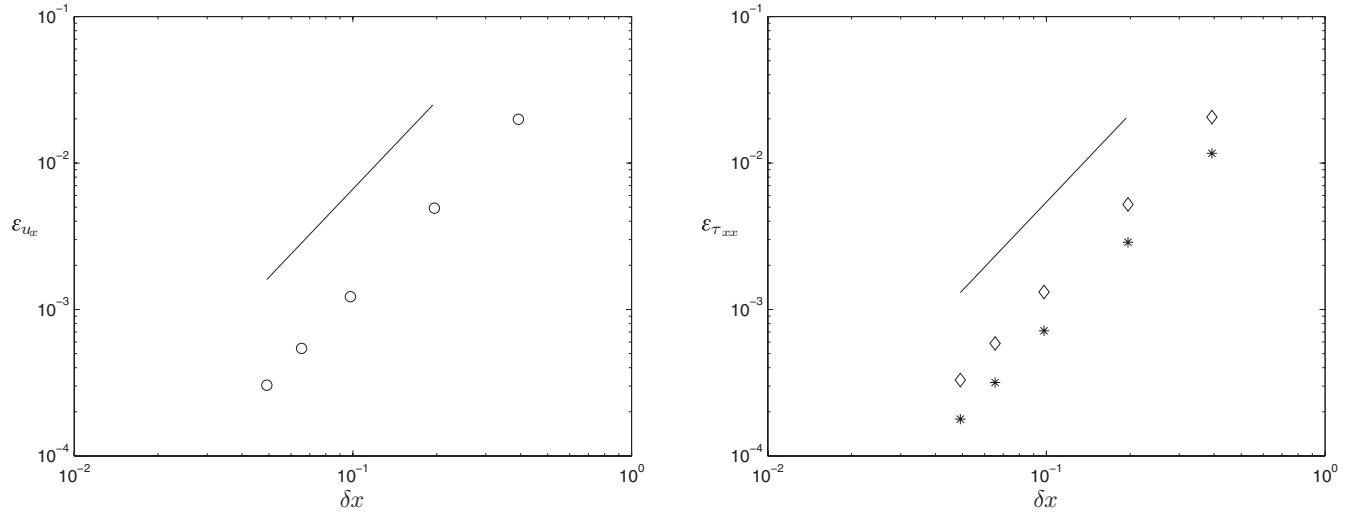

FIG. 4. The global relative errors of velocity u_x (left) and shear stress τ_{xx} (right) with different grid sizes ($\delta x = 2\pi/16,\ 2\pi/32,\ 2\pi/64,\ 2\pi/96$, and $2\pi/128$). $\diamond$ and $*$ are the results including and without including the forcing term effect, respectively; the slope of the line is 2, indicating a second-order accuracy of the multiple-relaxation-time lattice Boltzmann equation in computing velocity and shear stress.

As seen from this figure, the velocity and shear stress obtained by the MRTLBE are also second-order accurate in the lattice spacing δx or equivalently Ma [Eq. (52)] at such a critical Reynolds number.

Finally, we also give a special discussion of the relaxation factor s_ν because of its great influence on the accuracy of the lattice Boltzmann equation [20,34]. Following the method proposed in the previous work [20], the Reynolds number and Mach number are first specified at some reasonable values without changing the physics of the problem, and then according to Eq. (52), one can study the effect of the relaxation factor s_ν by changing the grid number. Some numerical simulations with different relaxation factors or equivalently grid numbers are conducted, and the results are presented in Fig. 6.

When the Mach number is small enough (for example, Ma $= 0.003$ or 0.03), the errors of the velocity and shear stress shown in Fig. 6 decrease with decrease of the relaxation factor s_ν; the reason is that a smaller s_ν leads to a larger grid number (or smaller δx), and also to more accurate results. However, the effect of the relaxation factor s_ν is relatively small for a large Mach number (Ma $= 0.3$); this may be because the error induced by a smaller s_ν at a large Mach number is compensated by a higher grid resolution. From the results in Fig. 6 we can also find that the Mach number should be small enough if one wants to obtain more accurate results.

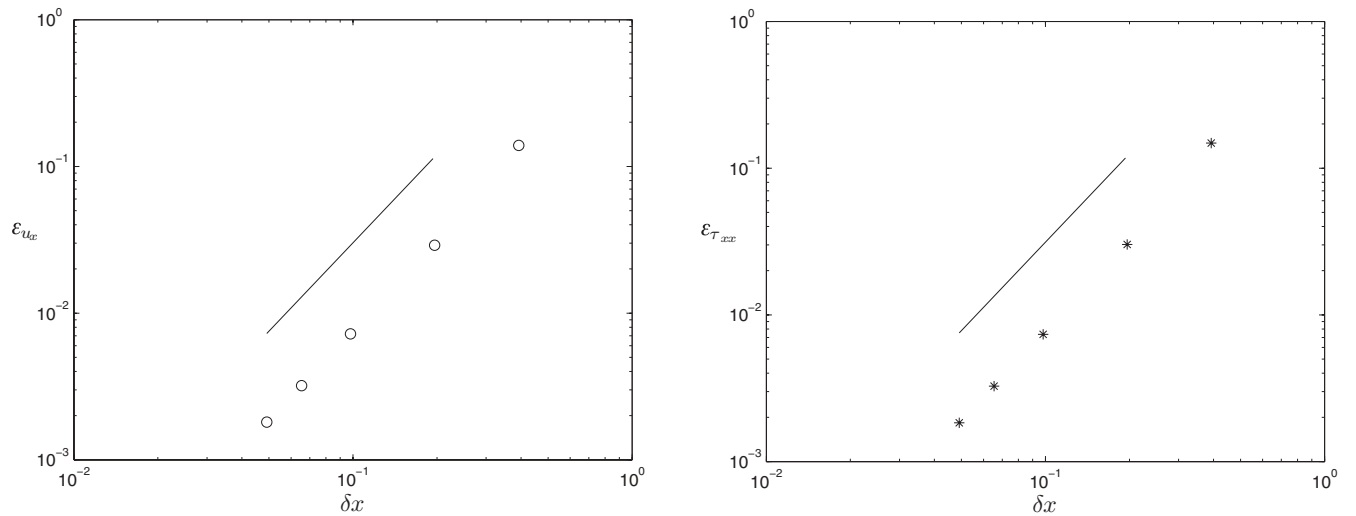

FIG. 5. The global relative errors of the velocity u_x (left) and shear stress τ_{xx} (right) with different grid sizes ($\delta x = 2\pi/16,\ 2\pi/32,\ 2\pi/64,\ 2\pi/96$, and $2\pi/128$). The slope of the line is 2, indicating that the shear stress derived from the multiple-relaxation-time lattice Boltzmann equation is second-order accurate.

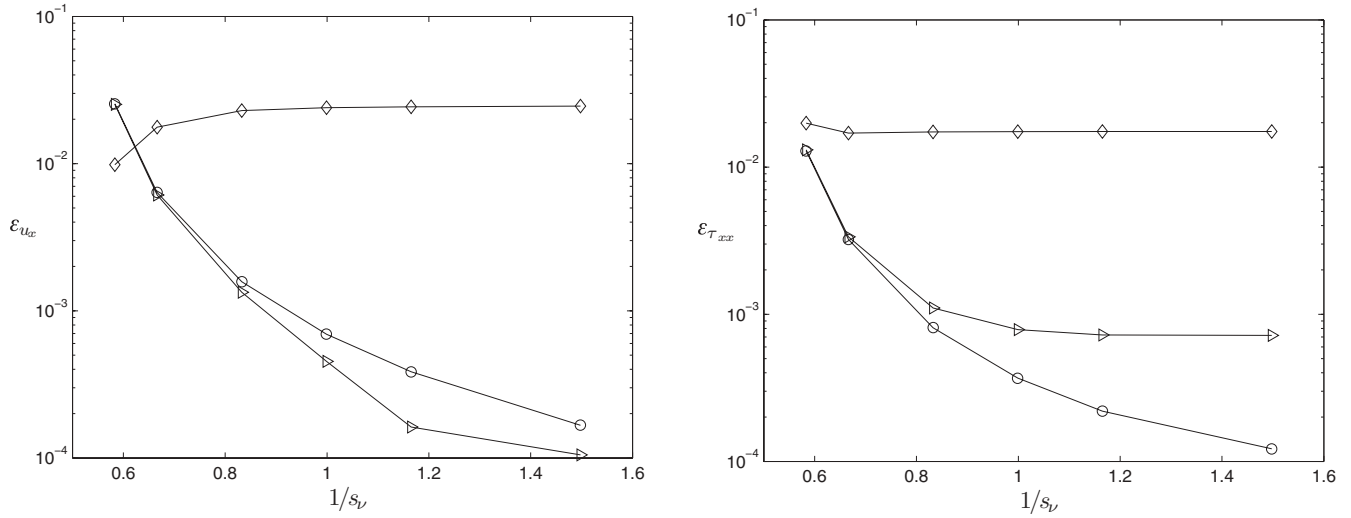

FIG. 6. The global relative errors of the velocity u_x (left) and shear stress τ_{xx} (right) with different relaxation factors (○, Re = 1, Ma = 0.003; ▷, Re = 10, Ma = 0.03; ◇, Re = 100, Ma = 0.3).

B. The forcing term effect in the multiple-relaxation-time lattice Boltzmann equation on the shear stress or strain rate tensor

To test the forcing term effect on the shear stress or the strain rate tensor, the problem of two-phase Poiseuille flow in a two-dimensional channel is adopted since one can easily obtain its theoretical solution [16]. The problem under consideration is illustrated in Fig. 7, where the flow is driven by an external force $\mathbf{F} = (\rho G, 0)$ (G is a constant) and assumed to be periodic in the x direction; the length (L) and height (H) of the channel are set to be 1.0. Following the work of Gross *et al.* [16], the theoretical solution for the shear stress can be derived,

$$\tau_{xy}(y) = -G\int_0^y \rho(y')dy' + C = \tilde{\tau}_{xy}(y) + C, \qquad (53)$$

where C is a constant and is given by

$$C = -\frac{\int_0^H \frac{\tilde{\tau}_{xy}(y')}{\rho(y')}dy'}{\int_0^H \frac{1}{\rho(y')}dy'}. \qquad (54)$$

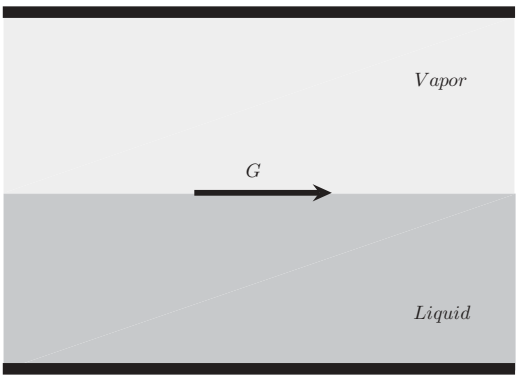

FIG. 7. Configuration of two-dimensional two-phase Poiseuille flow driven by a constant acceleration G.

To simulate two-phase Poiseuille flow, the Shan-Chen (SC) single-component multiphase lattice Boltzmann equation coupled with the MRT model (see Refs. [27,35] for details) is used for its simplicity. In the following simulations, the interaction strength G_{int} in the SC multiphase model is fixed to be -5.0, the equilibrium densities of liquid and vapor are 1.8884 and 0.1194 by including the interaction between the fluid and the solid wall. The parameter G and the lattice size are set to be 1.0×10^{-6} and 64×64, and the elements of the relaxation matrix $\mathbf{S}$ are given as $s_\rho = s_j = 0.0$, $s_e = s_\varepsilon = s_\nu = 1.1$, and $s_q = 1.9$. We present numerical results for the shear stress including and without including the forcing term effect in Fig. 8.

As seen from this figure, the numerical result agrees well with the theoretical solution once the forcing term effect is included. On the contrary, if the forcing term effect is not incorporated into the computation of the shear stress, the numerical result will present a serious oscillation at the interface between liquid and vapor and deviate from the theoretical solution.

To measure the deviation of the shear stress between analytical solutions and numerical results quantitatively, we also carried out numerical simulations under different interaction strengths (G_{int}), and present the global relative errors in Table I. As shown in this table, the forcing term indeed has a

TABLE I. The global relative errors of shear stress τ_{xy} between analytical solutions and numerical results. $\mathcal{E}^*_{\tau_{xy}}$ is the global relative error without including the forcing term effect, and ρ_v and ρ_l are the vapor and liquid densities.

G_{int}	ρ_v	ρ_l	$\mathcal{E}_{\tau_{xy}}$	$\mathcal{E}^*_{\tau_{xy}}$
−4.5	0.2330	1.4704	5.0042×10^{-4}	0.3266
−4.8	0.1560	1.7313	4.8377×10^{-4}	0.3756
−5.0	0.1194	1.8884	6.1021×10^{-4}	0.3966
−5.4	0.0670	2.1794	6.1784×10^{-4}	0.4234

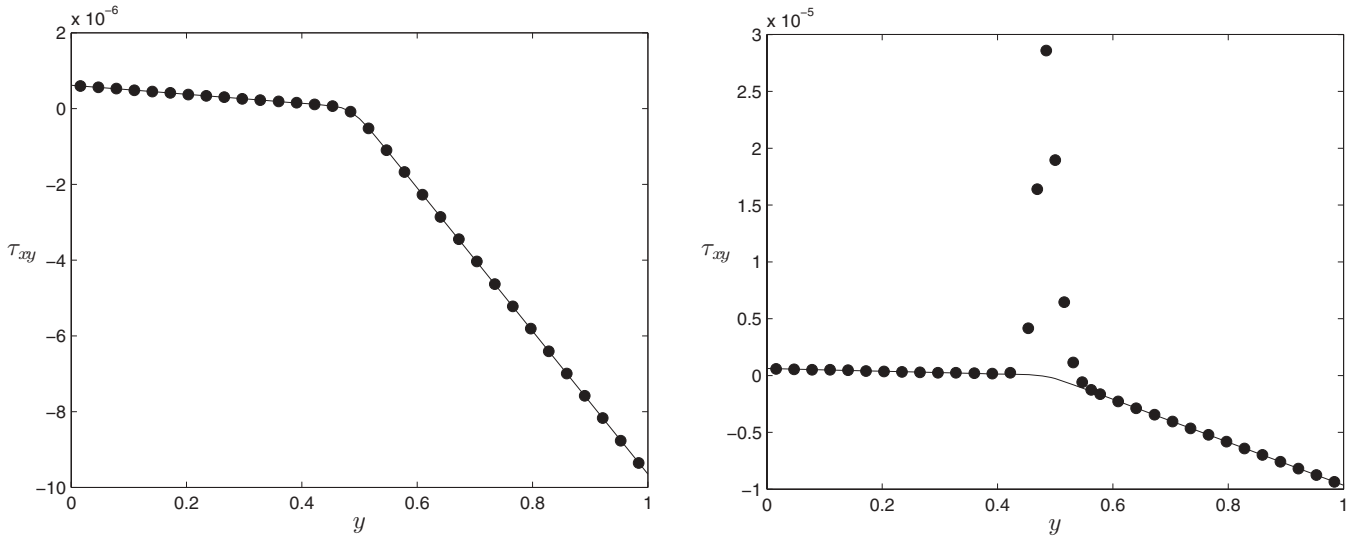

FIG. 8. The distribution of the shear stress component τ_{xy} in the y direction; left, τ_{xy} including the forcing term effect; right, τ_{xy} without including the forcing term effect (solid lines, theoretical results; symbols, numerical results).

very serious effect on the shear stress and must be included in practical computation.

IV. CONCLUSIONS

In this paper, the effect of the forcing term in the multiple-relaxation-time lattice Boltzmann equation on the shear stress and the strain rate tensor is studied. The theoretical analyses and numerical simulations demonstrate that the proposed scheme [Eqs. (31) and (30)] in computing the shear stress and the strain rate tensor is also second-order accurate in space. We further show that the effect of the forcing term is significant and must be included in calculating the shear stress or the strain rate tensor with the nonequilibrium part of the distribution function. Based on the advantages of the MRTLBE and the role of the shear stress and the strain rate tensor in practice, the present work may promote the MRTLBE in studying the blood flows, non-Newtonian flows, and multiphase flows, to name but a few.

ACKNOWLEDGMENTS

The authors thank anonymous referees for their valuable comments and suggestions which improved the quality of the present work. One of the authors (Z.C.) is indebted to Professor Zhaoli Guo, Professor Baochang Shi, and Markus Gross for their useful discussions. The work described in this paper was supported by a grant from the Research Grants Council of the Hong Kong Special Administrative Region, China (Project No. 62311). Z.C. is also financially supported by the National Natural Science Foundation of China (Grant No. 51006040), the Hong Kong Scholar Program, and the National Science Fund for Distinguished Young Scholars of China (Grant No. 51125024).

[1] R. Benzi, S. Succi, and M. Vergassola, Phys. Rep. **222**, 145 (1992).
[2] S. Chen and G. D. Doolen, Annu. Rev. Fluid Mech. **30**, 329 (1998).
[3] S. Succi, *The Lattice Boltzmann Equation for Fluid Dynamics and Beyond* (Oxford University Press, Oxford, 2001).
[4] C. K. Aidun and J. R. Clausen, Annu. Rev. Fluid Mech. **42**, 439 (2010).
[5] S. Gabbanelli, G. Drazer, and J. Koplik, Phys. Rev. E **72**, 046312 (2005).
[6] J. Boyd, J. M. Buick, and S. Green, Phys. Fluids **19**, 093103 (2007).
[7] M. Yoshino, Y. Hotta, T. Hirozane, and M. Endo, J. Non-Newtonian Fluid Mech. **147**, 69 (2007).
[8] A. Vikhansky, J. Non-Newtonian Fluid Mech. **155**, 95 (2008).
[9] Z. Chai, B. Shi, Z. Guo, and F. Rong, J. Non-Newtonian Fluid Mech. **166**, 332 (2011).
[10] M. Krafczyk, M. Cerrolaza, M. Schulz, and E. Rank, J. Biomech. **31**, 453 (1998).
[11] A. M. Artoli, A. G. Hoekstra, and P. M. A. Sloot, J. Biomech. **39**, 873 (2006).
[12] F. J. Rybicki, S. Melchionna, D. Mitsouras, A. U. Coskun, A. G. Whitmore, M. Steigner, L. Nallamshetty, F. G. Welt, M. Bernaschi, M. Borkin, J. Sircar, E. Kaxiras, S. Succi, P. H. Stone, and C. L. Feldman, Int. J. Cardiovasc. Imaging **25**, 289 (2009).
[13] J. C. Lasheras, Annu. Rev. Fluid Mech. **39**, 293 (2007).
[14] D. M. Sforza, C. M. Putman, and J. R. Cebral, Annu. Rev. Fluid Mech. **41**, 91 (2009).
[15] P. Sagaut, *Large Eddy Simulation for Incompressible Flows* (Springer, Berlin, 2006).
[16] M. Gross, N. Moradi, G. Zikos, and F. Varnik, Phys. Rev. E **83**, 017701 (2011).

[17] R. B. Bird, G. Dai, and B. J. Yarusso, Rev. Chem. Eng. **1**, 1 (1982).
[18] R. P. Chhabra and J. F. Richardson, *Non-Newtonian Flow and Applied Rheology* (Elsevier, Oxford, 2008).
[19] A. J. C. Ladd and R. Verberg, J. Stat. Phys. **104**, 1191 (2001).
[20] T. Krüger, F. Varnik, and D. Raabe, Phys. Rev. E **79**, 046704 (2009); **82**, 025701 (2010).
[21] U. Frisch, B. Hasslacher, and Y. Pomeau, Phys. Rev. Lett. **56**, 1505 (1986).
[22] X. He and L. S. Luo, Phys. Rev. E **55**, R6333 (1997); **56**, 6811 (1997).
[23] Y. H. Qian, D. d'Humires, and P. Lallemand, Europhys. Lett. **17**, 478 (1992).
[24] D. d'Humières, in *Rarefied Gas Dynamics: Theory and Simulations*, Vol. 159 of Progress in Astronautics and Aeronautics, edited by B. D. Shizgal and D. P. Weave, (AIAA, Washington, DC, 1992), pp. 450-458.
[25] P. Lallemand and L.-S. Luo, Phys. Rev. E **61**, 6546 (2000).
[26] L.-S. Luo, W. Liao, X. Chen, Y. Peng, and W. Zhang, Phys. Rev. E **83**, 056710 (2011).
[27] Z. Yu and L.-S. Fan, Phys. Rev. E **82**, 046708 (2010).
[28] Z. L. Guo and C. G. Zheng, Int. J. Comput. Fluid Dyn. **22**, 465 (2008).
[29] Z. Chai, B. Shi, Z. Guo, and J. Lu, Commun. Comput. Phys. **8**, 1052 (2010).
[30] Z. Guo, C. Zheng, and B. Shi, Phys. Rev. E **65**, 046308 (2002).
[31] C. Pan, L.-S. Luo, and C. T. Miller, Comput. Fluids **35**, 898 (2006).
[32] H. Yu, L.-S. Luo, and S. S. Girimaji, Comput. Fluids **35**, 957 (2006).
[33] O. Malaspinas, N. Fiétier, and M. Deville, J. Non-Newtonian Fluid Mech. **165**, 1637 (2010).
[34] D. J. Holdych, D. R. Noble, J. G. Georgiadis, and R. O. Buckius, J. Comput. Phys. **193**, 965 (2004).
[35] X. Shan and H. Chen, Phys. Rev. E **47**, 1815 (1993); **49**, 2941 (1994).